Mendez-Romero, D. & Garcia, M. J. F. G. (2018). Simpler Multipath Detection for Vehicular OFDM Channel Tracking. *IEEE Transactions on Vehicular Technology*, 67(11), pp. 10752–10759.

DOI: 10.1109/tvt.2018.2868445

Simpler Multipath Detection for Vehicular OFDM Channel Tracking

Diego Méndez-Romero, M. Julia Fernández-Getino García, *Member, IEEE*

***Abstract*—The ever increasing requirements in wireless communications have led to the search for unexploited correlations which could improve channel estimation and tracking. Kalman filtering (KF) has been proposed to exploit several such correlations, e. g. the time correlation in each tap in a multipath channel. When making full use of this correlation, however, a capital disadvantage of KF is its weak performance in the face of a significant, occasional non-linearity, such as the potential birth of a new tap in a multipath channel or an active tap's death. These non-linearities are typical for vehicular applications. So far, solutions proposed to this birth-death nonlinearity problem have been shown to be computationally prohibitive. In this work, a simplified detection framework is introduced and a computationally inexpensive Simplified Maximum a Posteriori (SMAP) estimator is derived. Under low to medium SNR conditions, simulations show the channel tracking error can be approximately halved (vs. simple KF) by this novel estimator in Orthogonal Frequency Division Multiplexing (OFDM) systems.**

***Index Terms*—OFDM, Kalman Filtering, vehicular, high-mobility, path birth-death, channel estimation.**

I. Introduction

Orthogonal Frequency-Division Multiplexing (OFDM) has spread quickly and it has become the base for many communication technologies, such as present-day Long-Term Evolution (LTE) systems. Recently, OFDM has also been proposed for providing broadband data services in high-mobility applications [1] such as high-speed rail [2]. Moreover, OFDM, in combination with other techniques such as filtering or spreading, is envisaged as the base for future waveforms in 5G scenarios.

In some OFDM environments, particularly in vehicular applications, it is necessary to track time-variant channels. For that purpose, one of the most frequently proposed techniques is Kalman filtering (KF) and its many adaptions and extensions [3].

Sometimes, some other information related to the channel is used to increase efficiency. In [4], for example, KF is used in combination with structure information of the channel impulse response (CIR) to estimate OFDM channels in a sparsity-aware mode. Forward-backward and forward KF are used in [5] in combination with data restriction information to greatly enhance estimation in a recursive manner; however, at a very large computional cost. The combination of KF, sparsity exploitation and recursion has also been recently proposed in [6] for OFDM estimation. Other published proposals include the use of an Extended Kalman Filter for MIMO-OFDM [7], a mixture KF for blind OFDM channel estimation [8], data-aided KF channel tracking [12] and the combination of pilots and KF [13], to name but just a few.

KF's advantage is its optimality as an estimator for linear problems; thus, if channel tracking can be approximated as a linear problem, the KF solution is near-optimal. However, as requirements grow and mobile communications spread into more dynamic channels, such as those of high-speed railways [14] in rugged terrain [15] or Unmanned Aerial Vehicles (UAVs) [16] in suburban/hilly terrain environments [17], random intermittent multipath components (MPCs) appear. The corresponding non-linearities, such as path birth and path death [18], could be catastrophic for KF-based estimation techniques. Accordingly, more powerful tap tracking techniques will be needed in the future.

Few in-depth analysis for the non-linear tracking problem have been published. So far, to our best knowledge, the only consistent proposal for tap tracking under birth-death conditions has been to use Random Set Theory (RST) models. In [9], [10], three possible RST-based estimators were compared; the so-called GMAP-III, which was proven to be the best performer by far, comes at a computationally prohibitive cost which renders it impracticable in real-world conditions. In this paper, a simpler birth-death detection paradigm is introduced which, in combination with KF, makes it feasible (i.e. computationally inexpensive) to approximately halve channel tracking error vs. bare KF under low to medium SNR conditions. This novel estimator is denoted Simplified Maximum a Posteriori (SMAP) estimator.

This paper is organized as follows. In Section II, the problem is formally stated. Then, a quick review of approaches to channel tracking and how to measure their quality is made in Section III. The proposed SMAP estimator is introduced in Section IV, and its simulated results are shown in Section V. Finally, conclusions are extracted in Section VI.

II. Statement of the problem

We consider an OFDM system employing N orthogonal subcarriers, transmitting OFDM symbols with a time duration T_{symb} and a sampling interval T_{samp}. It is assumed there is no out-of-band interference. Periodically, each subcarrier is used first for pilot symbols enabling channel estimation, and then for data transmission (through data blocks of fixed length M_{inf}). Each data block is preceded by K pilot symbols, so that the first K sent symbols are pilot symbols used to

The authors are with the Department of Signal Theory and Communications, Universidad Carlos III de Madrid (Spain). E-mail: {dmendez, mjulia}@tsc.uc3m.es.

estimate the channel (by averaging over K); this channel estimation will be considered "valid" and will be used for the whole subsequent M_{inf}-symbol data block transmission. Channel changes will be tracked only once every estimation period $T_{est} = (K + M_{inf}) \cdot T_{symb}$, since a certain channel stationarity within each estimation period can be assumed due to its coherence time and, accordingly, channel changes can be reasonably modeled as occurring at the beginning of each estimation period.

If $k = \{1, ..., K\}$ is the pilot symbol index in the pth estimation period, then the received signal, which is the input for channel estimation, can be given in vector form as:

$$\mathbf{y}_{p,k} = \mathbf{D}_{p,k}\mathbf{F}_p\mathbf{h}_p + \mathbf{z}_{p,k} \tag{1}$$

where $\mathbf{y}_{p,k} = [y_{p,1,k}, ..., y_{p,N,k}]^T$, each $y_{p,n,k}$ (for $n = \{1, ..., N\}$) represents the nth subcarrier observation sample at time $t_{p,k} = (p-1) \cdot T_{est} + (k-1) \cdot T_{symb}$; $\mathbf{D}_{p,k} = diag(d_{p,1,k}, ..., d_{p,N,k})$,with $d_{p,n,k}$ the training data on the nth pilot subcarrier at time $t_{p,k}$; $\mathbf{z}_{p,k} = [z_{p,1,k}, ..., z_{p,N,k}]$, with $z_{p,n,k}$ representing the zero-mean complex Gaussian additive noise having variance σ_z^2; if $l = \{1, ..., L(pT_{est})\}$ and $L(pT_{est})$ is the number of active paths, then $\mathbf{h}_p = [h_1(pT_{est}), ..., h_{L(pT_{est})}(pT_{est})]^T$, with $h_l(pT_{est})$ the complex gain of the lth path at time p, which, as previously explained, will be assumed constant for the duration of the estimation period; and

$$\{\mathbf{F}_p\}_{n,l} = e^{-j2\pi n \cdot \frac{\tau_l(pT_{est})}{NT_{samp}}} \tag{2}$$

where $\tau_l(pT_{est})$ is the delay of the lth path during the pth interval.

Clearly, since each data block is preceded by K pilot symbols, the received signal including reception of all K pilot symbols will be the matrix $\mathbf{Y}_p = [\mathbf{y}_{p,1}, ..., \mathbf{y}_{p,K}]$. A guard time, named cyclic prefix, T_{CP} is reserved between OFDM symbol transmissions, so that $T_{symb} = NT_{samp} + T_{CP}$. It is assumed that the multipath delay spread is smaller than T_{CP}.

Moreover, the active path gains are assumed to follow an underlying Linear Gauss-Markov (LGM) model [3]. For ease of notation, $a_p^{(l)} = h_l(pT_{est})$ will represent the lth path gain at time p. Provided that the lth path is active and remains so, the probability density function (pdf) for $a_p^{(l)}$ would be given by both following equations:

$$f(a_1^{(l)}) = N(a_1^{(l)}; 0, \sigma_{h_l}^2) \tag{3}$$

$$f(a_p^{(l)}|a_{p-1}^{(l)}) = N(a_p^{(l)}; \lambda a_{p-1}^{(l)}, (1-\lambda^2)\sigma_{h_l}^2) \tag{4}$$

where $\sigma_{h_l}^2$ is the average energy of the lth path and λ is the temporal self-correlation of each active path gain. However, notice that, if the lth path is not active (because it has "died"), then $h_l(pT_{est})$=0, i.e. path gain equals zero. Each active path has a probability P_{death} of becoming inactive; each inactive path has a probability P_{birth} of becoming active.

The problem under consideration can now be formulated as follows: given the observations (1), determine a computationally inexpensive causal estimator $\hat{\mathbf{h}}_p$ for $\mathbf{h}_p$, relying upon $\{\mathbf{Y}_{1:p}\}$. Since "computationally inexpensive" may be too vague a term, a slightly different, more precise formulation of the problem would be: determine the $simplest$ causal estimator for $\mathbf{h}_p$ exploiting path self-correlation to the extent of getting $most$ of the theoretically maximum possible reduction in Channel Tracking Mean Squared Error (CTMSE), defined as:

$$CTMSE \triangleq ||\sum_p \hat{\mathbf{h}}_p - \mathbf{h}_p||_2^2 \tag{5}$$

where $||\cdot||_2$ denotes the Euclidean norm.

III. Channel tracking

A. Linear Gauss-Markov (LGM) models

Let us consider a LGM model where all paths are active and they follow (3) and (4). These LGM models have been previously used in the literature (e.g. in [9], [10]) and they make it possible to derive a computationally inexpensive, optimal estimation through Kalman filtering. However, they are ideal channels whose behaviour may or may not approximate specific real channels. In this regard, a severe disadvantage is that, since they are perfectly linear, they don't allow for jumps.

B. KF-based approaches

Under a LGM model, a KF-based approach can be easily implemented. Kalman filtering is an algorithm weighting optimally two information sources: a theoretical one (in our case, the LGM channel model) and another one based on noisy measurements. The Least-Squares (LS) channel estimation, $\hat{\mathbf{a}}_p^{LS}$, can be interpreted as a noisy measurement of the true channel $\mathbf{a}_p = [a_p^{(1)}, ..., a_p^{(L)}]^T$:

$$\mathbf{u}_p \triangleq \hat{\mathbf{a}}_p^{LS} = \mathbf{a}_p + \mathbf{v}_p \tag{6}$$

where $\mathbf{v}_p = [v_p^{(1)}, ..., v_p^{(L)}]^T$ is the measurement noise and $\mathbf{u}_p = [u_p^{(1)}, ..., u_p^{(L)}]^T$ will be used for ease of notation. Since path independence is being assumed, this translates into L scalar equations. Thus, a bank of independent Kalman filters could be used to track the whole channel, whereby each Kalman filter would receive the LS-estimated tap gain and would compute the corresponding KF tap estimation, $\hat{u}_p^{(l)}(+)$, and also the expected path gain at time $p+1$, the so-called Kalman prediction, $\hat{u}_{p+1}^{(l)}(-)$. Please note that the $(-)$ sign denotes prediction while $(+)$ denotes estimation. This distinction is important (algorithms are different) and relevant to this paper.

This KF approach is optimal when non-linearities are absent. However, the disappearance and reapparance of paths (i.e. the real channel "jumping" in a way the perfect LGM model cannot fit) introduce a severe nonlinear distortion and KF performance degrades catastrophically.

C. RST-based approaches

RST-based approaches have proven that, under birth-death conditions, a very good estimator is the so-called GMAP-III, which essentially adds a death-birth detector before the KF step. Thus, you first detect which paths are active, and then

you estimate active paths' gains. The GMAP-III estimator was proposed in [9] with the following definition:

$$\text{GMAP-III}: \begin{cases} \widehat{\pi(\mathcal{H}_p)} = \arg\max_{\pi(\mathcal{H}_p)} f_{\pi(\mathcal{H}_p)|\mathcal{Y}_{1:p}}(\pi(\mathcal{H}_p)|\mathcal{Y}_{1:p}), \\ \widetilde{\mathbf{h}}_p = \int_{\mathbb{R}^{2|\widehat{\pi(\mathcal{H}_p)}|}} \mathbf{h}_p f_{\mathbf{h}_p|\mathcal{Y}_{1:p}}(\mathbf{h}_p|\mathcal{Y}_{1:p}) d\mathbf{h}_p \end{cases} \tag{7}$$

where $f(\cdot)$ represents a pdf and

$$f_{\pi(\mathcal{H}_p)|\mathcal{Y}_{1:p}}(\pi(\mathcal{H}_p)|\mathcal{Y}_{1:p}) = \int_{\pi'(\mathcal{H}_p)} f(\mathcal{H}_p|\mathcal{Y}_{1:p}) \delta\mathcal{H}_p \tag{8}$$

(For further details on notation, see [9]). However, death-birth detection under the RST framework can be difficult to handle and computationally prohibitive, e.g. in [9], death-birth detection is done through a 10,000-particle filter that approximates (7). It is evident that a much simpler, suboptimal estimator is required for practical applications. Such an estimator will be proposed in Section IV, but, firstly, a measurement of its quality will be introduced in the following Section.

D. Measuring the quality of simpler estimators

Our objective is to reduce CTMSE as defined in (5). What is the theoretically maximum possible reduction in CTMSE when using some given birth-death information?

First, let us consider Fig. 1 to see how path birth-death information could be used in practice. Following the notation for (6), Fig. 1 starts with the LS channel estimation, $\hat{\mathbf{a}}_p^{LS}$, having its individual path components extracted and fed into individual path birth-death detectors. These detectors are like switches and are represented as such in Fig. 1: on birth detection, the lth LS path estimation is fed into the lth KF, which starts tracking and provides $\hat{u}_p^{(l)}(+)$, the lth estimated path gain (not to be confused with $\hat{u}_p^{(l)}(-)$, which is a prediction done at time $p-1$); on death detection, however, the lth estimated path gain is put to zero until the next time the lth path is detected to be reborn. Since the problems of birth-death detection, on the one hand, and active-path tracking, on the other hand, are separable in nature, the maximum reduction in CTMSE is obtained when, for each path, an optimal birth-death detector is connected to a KF.

Now, let us suppose perfect information on the active/inactive status of each tap was available. What would the theoretically maximum possible reduction in CTMSE be when using this perfect birth-death information? Death-birth detectors would then be always right, and looking into this ideal case, henceforth the Ideal Switching System (ISS), could provide useful information about the problem and the quality of different solutions to it.

Thus, the ISS is the system drawn in Figure 1 when death/birth detectors detect 100% of births and 100% of deaths, with no false birth/death detection. It is also possible to easily define an x%-degraded Ideal Switching System (IIS-x%), which is a switching system detecting x% of births and x% of deaths, with no false birth/death detection. These degraded ISS were simulated for the problem at hand (for more details, see Section V) and Table 1 shows the % reduction (vs. the LS method, i.e., no KF) these near-optimal ISS devices could achieve, as measured in CTMSE, for different

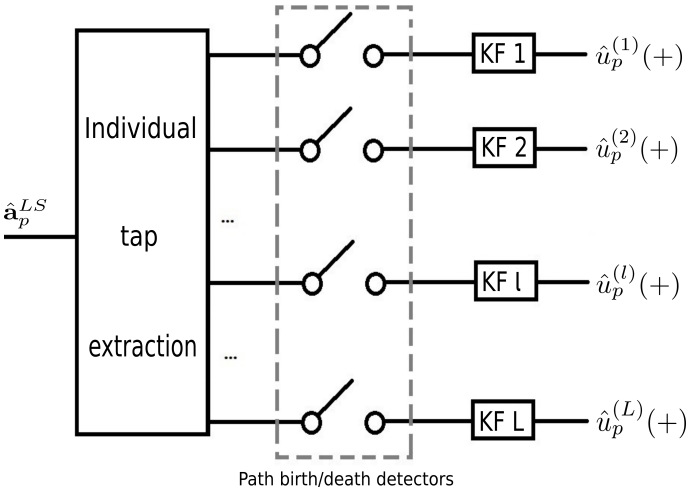

Fig. 1. Tap birth/death detectors and KF bank arrangement.

TABLE I
% REDUCTION IN CTMSE FOR DIFFERENTLY DEGRADED ISS VS. LS ESTIMATION.

SNR [dB]	ISS	ISS-99.9%	ISS-99.5%	ISS-99%
8.5	72.84	72.46	69.35	66.52
11	70.16	68.86	64.81	59.14
13.5	65.40	63.75	56.81	45.77
16	56.93	53.83	40.59	23.77
18.5	41.81	35.29	8.72	-16.40

SNR values. A quick look at Table 1 makes it possible to conclude that ISS performance in terms of CTMSE degrades significantly even with minor reductions in the % of birth/death detections. For higher SNR, the degradation is so catastrophic that the conventional LS estimation performs better than a slightly degraded ISS (e.g. an ISS-99%, negative value in the bottom-right corner of Table 1). Do note, however, that the degraded ISS greatly improves estimation over conventional LS estimation for low-to-medium SNR levels.

These conclusions are also backed by Figure 2, which plots the degraded systems' performance in terms of CTMSE. This kind of plots let us establish a natural measure for an estimator's fitness in the context of the previously defined problem. Some estimator could be, for example, better than ISS-97% and worse than ISS-98%, meaning that it would be slightly better than a degraded ISS where detectors detected 97% of births and 97% of deaths, but not as good as a system detecting 98% of both.

It must also be noted that the performance of OFDM is sensitive to the existence of carrier frequency offset (CFO). However, there are numerous proposals in the literature for frequency synchronization in OFDM, based on specific headers or pilot sequences, which attain an adequate synchronization with negligible residual errors (refer to recent works [19], [20], [21]).

IV. Proposed scheme: SMAP estimator

A Bayesian-inspired estimator of $\mathbf{h}_p$ can be defined by using KF in combination with the three following heuristics for path

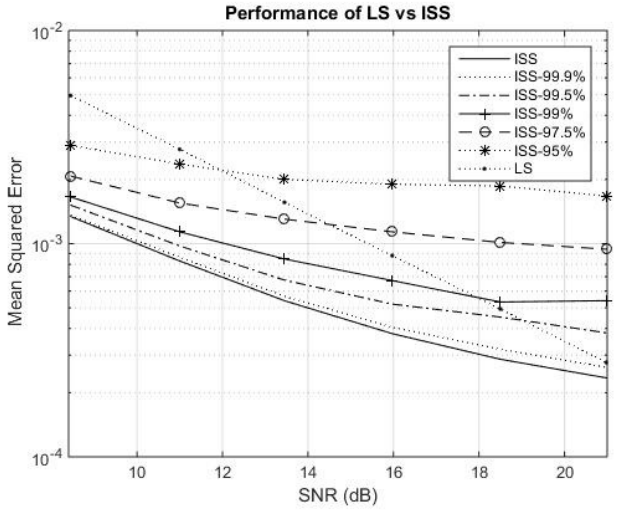

Fig. 2. Average CTMSE performance of LS vs. ISS and different x%-degraded ISS

birth-death detection: 1) detect death if the path gain jumps into approx. zero; 2) detect death if the path gain has slowly converged into approx. zero; 3) detect birth if the path gain is far from zero. These three rules can ultimately be simplified to three threshold comparisons, as shown in the three following Sections through simple theoretical derivations. The specific threshold parameter values can then be obtained empirically through precision simulations, as discussed and shown in Section IV.D.

A. Memoryless detection of large leaps into a narrow, zero-centered range

When the lth path is dead, its true gain is, by definition, zero. Thus, the observed gain is just the (Gaussian) noise. Hence, path gain measurement $u_p^{(l)}$ follows a Gaussian distribution:

$$u_p^{(l)}|l\,is\,dead \sim N(0, \sigma^2_{v^{(l)}}) \tag{9}$$

where $\sigma^2_{v^{(l)}}$ is the variance of path (measurement) noise $v_p^{(l)}$. On the other hand, if lth path is active, then its gain follows a Gaussian centered on the previously expected gain, $\hat{u}_p^{(l)}(-)$, the Kalman prediction computed at time $p-1$ (this is a feature of KF). Two variance sources can be identified for this Kalman prediction: measurement noise $\sigma^2_{v^{(l)}}$ and channel tap variance $(1-\lambda^2)\sigma_h^2$. Thus, it is convenient to consider

$$u_p^{(l)}|l\,is\,alive \sim N(\hat{u}_p^{(l)}(-), \sigma_A^2) \tag{10}$$

where

$$\sigma_A = q_A \cdot \sqrt{\sigma^2_{v^{(l)}} + (1-\lambda^2)\sigma_h^2} \tag{11}$$

and q_A is an error-minimizing positive threshold (as later explained in Section IV.D).

Let us assume that the path was alive at time $p-1$. Then, either path death happens at time p (with prior probability P_{death}) or the path will still be alive (with prior probability $1-P_{death}$). Thus, a maximum a posteriori criterium leads to detecting "death" whenever

$$P_{death} \cdot f(u_p^{(l)}|l\,is\,dead) > f(u_p^{(l)}|l\,is\,alive) \cdot (1-P_{death}) \tag{12}$$

where $f(\cdot)$ represents a pdf and the events "l is dead/alive" mean that the lth path is dead/alive, respectively. Note that this detector compares two scaled Gaussian pdfs, so an equivalent expression to (12) would be:

$$P_{death} \cdot \frac{1}{\sqrt{2\pi}\sigma^2_{v^{(l)}}} \cdot e^{-\frac{(u_p^{(l)})^2}{2\sigma^2_{v^{(l)}}}} > \frac{1}{\sqrt{2\pi}\sigma_A^2} \cdot e^{-\frac{(u_p^{(l)} - \hat{u}_p^{(l)}(-))^2}{2\sigma_A^2}} \cdot \cdot(1-P_{death}) \tag{13}$$

By taking logarithms and simple rearrangement, another equivalent expression can be found:

$$ln(\frac{P_{death}}{1-P_{death}}) > \frac{(u_p^{(l)})^2}{2\sigma^2_{v^{(l)}}} - \frac{(u_p^{(l)} - \hat{u}_p^{(l)}(-))^2}{2\sigma_A^2} \tag{14}$$

where $ln(\cdot)$ denotes the natural logarithm.

B. Memory detection of a sequence at a close range of zero

Let the lth path gain be active and close to zero (but never exactly zero, since it is active!) at time p, i.e. $0 \neq u_p^{(l)} \approx 0$; since large leaps are highly improbable as Gaussian outliers [11], let's assume that path gain will always stay close to zero at time $p+1$. (This is a reasonable assumption if done only for very short sequences, typically 2 or 3 succesive samples; it is in these short transitions where simple KF gets "confused" and needs most help). Thus, the active path is assumed to be close to zero, continously active and static, and the observed path gain is assumed to be just measurement noise (a reasonable assumption when path gain is very close to zero). Under these assumptions, the probability of having a sequence $\{|u_{p+1}^{(l)}|, ..., |u_{p+s}^{(l)}|\}$ of length s at any range $q_B \cdot \sigma_v$ from zero, such that the path is continously active and $\{|u_p^{(l)}|, ..., |u_{p+s}^{(l)}|\} < q_B \cdot \sigma_v$, is:

$$P_{seq\_in\_rge} = (1-P_{death})^s \cdot (1-2Q(q_B))^s \tag{15}$$

where $Q(\cdot)$ is the Q-function and q_B is any arbitrary threshold consistent with the aforementioned assumptions. Eq. (15) follows directly from the properties of the Gaussian distribution [11]. On the other hand, the probability of a path dying right before the sequence or during the sequence (and not being reborn afterwards) would be:

$$P_{dyi\_seq} = \sum_{i=0}^{s} (1-P_{death})^i \cdot P_{death} \cdot (1-P_{birth})^{s-i} \tag{16}$$

Thus, if the system is continuously monitoring the presence of sequences in this range, path death can be decided following a simplified maximum a posteriori criterium whenever:

$$P_{dyi\_seq} > P_{seq\_in\_rge} \tag{17}$$

Thus, after setting a single appropiate threshold q_B not too far from zero and a short enough sequence length s, path

death can be decided trivially when an $(s+1)$-long sequence $\{|u_p^{(l)}|, ..., |u_{p+s}^{(l)}|\} < q_B \cdot \sigma_v$ has been detected.

For example, if a sequence monitor for $q_B = \sigma^2_{v^{(l)}}/3$ and $s = 2$ is set up, then this detector would decide "dead" after a 3-long sequence $\{|u_p^{(l)}|, ..., |u_{p+s}^{(l)}|\} < q_B \cdot \sigma_{v^{(l)}} = \sigma^3_{v^{(l)}}/3$ per (17). Appendix A shows that, if assumptions are reasonable and hold true, the probability of having made the wrong decision is:

$$P_{err} = \frac{(1 - P_{death})^s \cdot (1 - 2Q(q_B))^s}{P_{aux} + (1 - P_{death})^s \cdot (1 - 2Q(q_B))^s} \tag{18}$$

where

$$P_{aux} = \sum_{i=0}^{s} (1 - P_{death})^i \cdot P_{death} \cdot (1 - P_{birth})^{s-i} \tag{19}$$

C. Birth detection

Birth detection could easily be implemented as a threshold detector that decides "alive" whenever $|u_p^{(l)}| > q_C \cdot \sigma_{v^{(l)}}$, for a certain threshold q_C. Even if P_{err} per (18) were too high (close to 0.5), a very sensitive birth detector (a very low q_C) would correct potential errors very early. Thus, detecting a path birth is a correct decision not only when a new path is created, but also when a path was wrongly detected as "dead".

Let's assume our birth detection happens immediately after having decided "path is dead" in the scenario described in Section IV.B. Since P_{err} in (18) is the probability of that previous decision having been wrong, and since noise can make an LS estimate of a dead path deviate outside a q_C range from zero with a probability $2Q(q_C)$, then the probability of correcting a previous error would be:

$$P_{corr} = P_{err} \cdot (1 - P_{death}) \cdot 2Q(q_C) \tag{20}$$

On the other hand, a new path could have been created (with prob. P_{birth}) if the previous decision ("dead path") was right (with prob. $1 - P_{err}$). For simplicity purposes, let's assume that newly created paths start at $|u_{p+1}^{(l)}| > q_C \cdot \sigma_{v^{(l)}}$. Thus, the probability of correctly detecting a new birth would be:

$$P_{birth\,det} = (1 - P_{err}) \cdot P_{birth} \tag{21}$$

A birth decision would be wrong if the path was erroneously detected as dead at time p but it has recently become dead at time $p + 1$ and noise puts it outside the detection limits, or when it was correctly detected as dead at time p and is still dead, but noise makes the observation sample shoot outside the detection limits:

$$P_{false\,det} = P_{err} \cdot P_{death} \cdot 2Q(q_C) + (1 - P_{err}) \cdot (1 - P_{birth}) \cdot 2Q(q_C) \tag{22}$$

Thus, a simplified maximum a posteriori criterium would decide "birth" whenever:

$$P_{corr} + P_{birth\,det} > P_{false\,det} \tag{23}$$

These expressions look cumbersome but, in fact, you only need them to obtain any appropiate q_C for which (22) holds true. Once a single appropiate threshold q_C is set, path birth can be decided trivially when $|u_p^{(l)}| > q_C \cdot \sigma_{v^{(l)}}$ has been detected. When birth is detected, the KF is restarted and the first estimate is the LS estimate.

D. Threshold parameter values

The system resulting from the three detection heuristics shown above and a connected KF block will be called "Simplified Maximum a Posteriori" (SMAP) estimator.

The proposed method, as suggested by the theoretical analysis in previous Sections, could have a positive performance independently from the specific choice of threshold values, provided that they reasonably fit the assumptions in Section IV. Even though results (in Section V) will show the system to be rather robust to variations in parameter value selection, it is convenient to fine-tune it by obtaining an optimal set of parameter values for q_A, q_B and q_C through simulations. Several strategies are legitimate for this purpose. A set of values could be optimised in terms of MSE reduction, BER/SER reduction, or a combination of performance and sensitivity. In Section V, an approach based on MSE reduction is implemented and a sensitivity analysis is performed. Simulation results back the theoretical derivations and the optimization strategy advocated here.

V. Simulation results

A system with $N_p = 3$ pilot subcarriers is considered, with $K = 8$ pilot symbols per subcarrier before data transmission. The average energy per pilot symbol, σ_s^2, is uniform, and a BPSK modulation scheme is assumed. Channel assumptions include a uniform multipath delay profile, multipath spread smaller than the guard time, and uncorrelated path gains. The overall channel energy is normalized to one. OFDM symbols were transmitted through a channel with $L_{max} = 3$, $P_{birth} = 0.05$ and $P_{death} = 0.05$. Threshold parameter values $q_A = 0.23$, $q_B = 0.30$ and $q_C = 0.62$ were obtained through simulation-based MSE optimization for $s = 1$ and form the basis for the simulation results shown here. Note that this prior optimization is always performed offline and, thus, it does not increase online computational complexity. This channel was then tracked for 200,000 estimations periods ($2 \cdot 10^5 \cdot T_{est}$). Individual paths were assumed to have the same average energy σ_h^2 over long periods and $\lambda = 0.999$. This choice of parameters makes it possible to compare the performance of the SMAP vs. the computationally heavier methods outlined in [9] and the KF system advocated in [13].

Fig. 3 shows the performance (in terms of CTMSE, as per (5)) of our proposed SMAP estimation vs. a scenario with perfect information (ISS), almost perfect information (ISS-99%) and a KF system. It can be seen that the SMAP estimator is very similar in performance to ISS-99%. This means the SMAP estimator gets most of the reduction attainable by an ISS, but with a trivially low computational cost, for low-to-medium SNR.

A measurement of SMAP's robustness in the face of model uncertainty can be provided by setting random thresholds q_A, q_B and q_C extracted from Gaussians centered on the previously determined optimal values. Fig. 4 shows simulation results for several standard deviation σ values, e.g. $\sigma_{\%} = 40\%$ means SMAP is not used now with optimal thresholds, but rather with several different random threshold triplets taken from Gaussians: $q_C \sim N(0.62, \sigma = 0.62 \cdot 0.40 = 0.248)$,

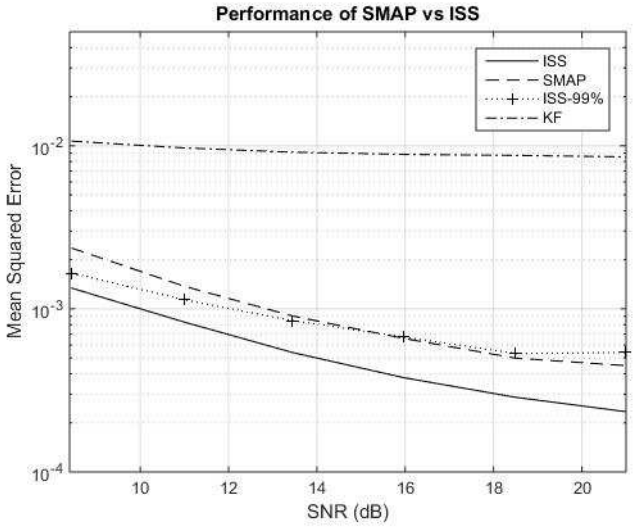

Fig. 3. Average CTMSE performance of proposed SMAP vs. ideal systems and KF

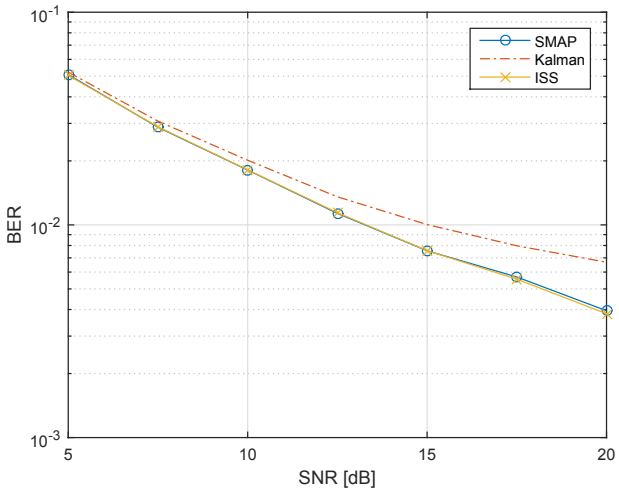

Fig. 5. BER performance of proposed SMAP vs. ideal system (ISS) and KF

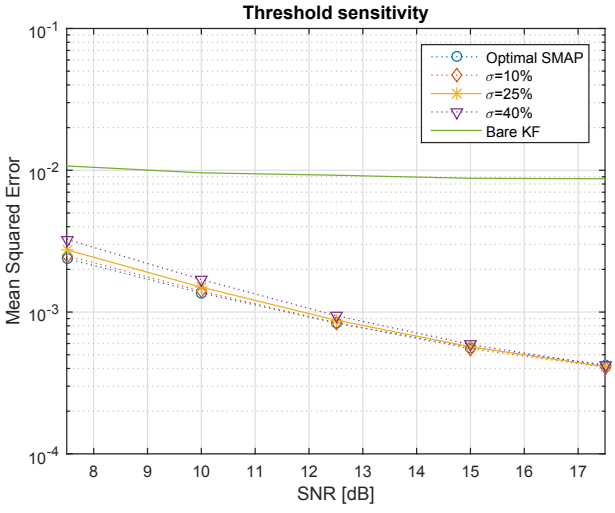

Fig. 4. Average CTMSE performance of SMAP with differently-deviated random thresholds vs. KF and optimal-threshold SMAP

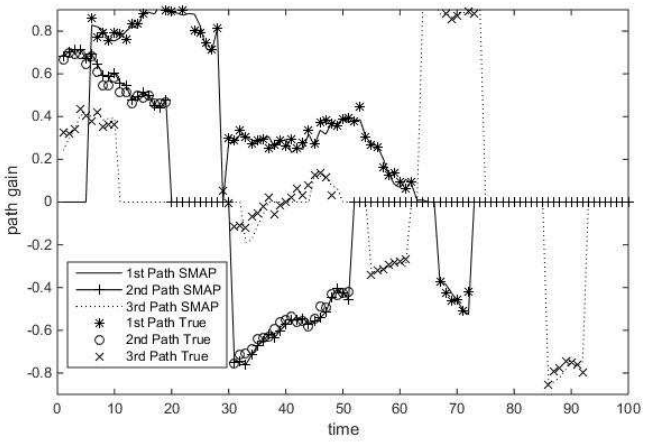

Fig. 6. SMAP estimation for L=3, SNR=15 dB.

etc. In this particular simulation, 10 such random triplets were extracted for each σ and SNR level. It is apparent from Fig. 4 that large deviations result in smaller changes in CTMSE, especially when compared to bare Kalman. Thus, the use of a SMAP structure is shown to be a larger contributor to error reduction than the use of perfect thresholds in that SMAP structure. This low sensitivity to threshold deviations means SMAP is robust to some extent when facing some uncertainty in model parameters.

Fig. 5 shows the bit-error-rate (BER) performance of SMAP vs. the ideal system (ISS) and a KF system. This considers all samples when at least one path is active (channel energy at least 5% of average channel energy), thus ignoring samples when all channel taps are zero and communication must be unfeasible. It must be noted that BER values were obtained without considering any channel coding scheme which would improve system performance. Results are unambiguous: the BER curve for SMAP matches the one for the ideal system (ISS) and both of them have a significant positive gap vs. bare KF.

Now let us take a closer look at Figs. 6-7, which show the estimated path gain in SMAP and KF systems, respectively, for a signal-to-noise ratio SNR $\triangleq \sigma_s^2/\sigma_z^2 = 15$ dB. These figures support the thesis, already advanced in [9], that a KF operating on L_{max} paths suffers from a transient effect from path death/birth. The proposed SMAP estimation adapts more quickly to those non-linearities. This superior performance when a path disappears or a new path is born can also be seen for SNR $= 9$ dB in Figs. 8-9 and for SNR = 21 dB in Figs. 10-11.

Moreover, this superior performance does not come at the expense of a prohibitively high computational cost. On the contrary, each path detector uses only the three computationally inexpensive threshold comparisons outlined in Section IV to achieve an error reduction matching that of a close-to-perfect path death/birth detection (ISS-99%).

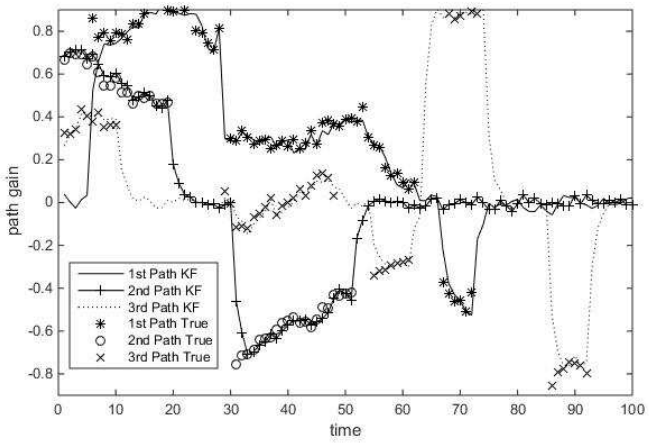

Fig. 7. KF estimation for L=3, SNR=15 dB.

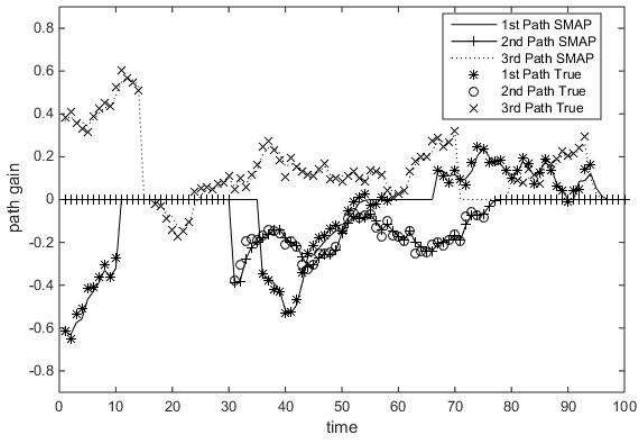

Fig. 10. SMAP estimation for L=3, SNR=21 dB.

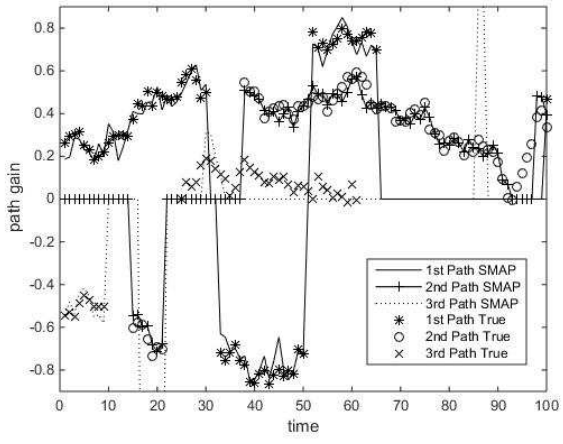

Fig. 8. SMAP estimation for L=3, SNR=9 dB.

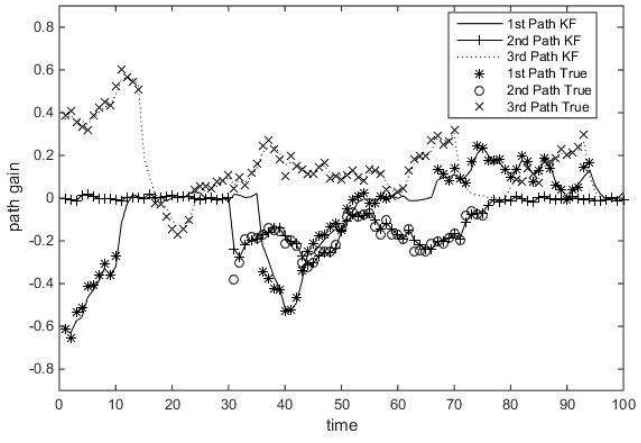

Fig. 11. KF estimation for L=3, SNR=21 dB.

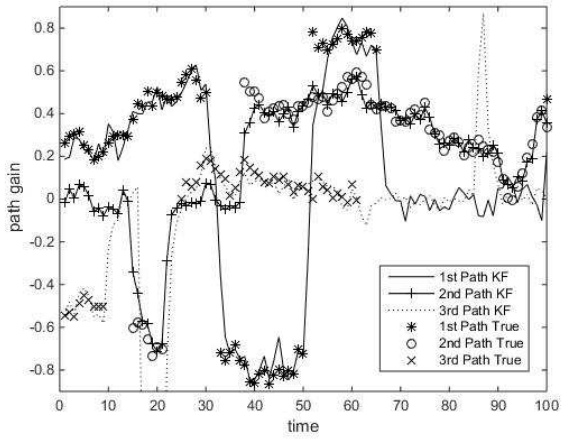

Fig. 9. KF estimation for L=3, SNR=9 dB.

VI. Conclusion

A simplified framework for the birth-death nonlinearity problem has been introduced. A computationally inexpensive, threshold-based estimator was derived. Simulations have shown this estimator greatly reduces channel tracking error in the target SNR range at a very small computational cost, thus outperforming previously known systems.

Appendix A
Derivation of error probability in memory death detection

A sequence of length $s+1$ at any range $q_B \cdot \sigma_v$ from zero, $\{|u_p^{(l)}|, ..., |u_{p+s}^{(l)}|\} < q_B \cdot \sigma_v$, could represent any of the following four events: A_1, all true gains are outside the zero-centered tunnel but measurement noise put estimated gains into the tunnel; A_2, all true gains are inside the tunnel; A_3, the path dies (gain goes to 0) and it is not reborn later in the sequence; A_4, the path dies but it is reborn shortly afterwards (in the s-sized sequence). The proposed approach in this paper is to assume that the probability $P(A_1) \approx 0$, since A_1 is covered by the memoryless detector and otherwise it could

only happen due to succesive large Gaussian leaps (succesive outliers of negligible probability) or due to short leaps from true gains which were close to the tunnel (which amount to a negligible increase in CTMSE if death is wrongly detected). Thus, the false detection probability when using the memory death detector (Section IV.B) would be:

$$P_{err} = \frac{P(A_2) + P(A_4)}{P(A_2) + P(A_3) + P(A_4)} \quad (24)$$

Under the assumptions outlined in IV.B, the probabilities for events A_2 and A_3 were derived as $P(A_2) = (1 - P_{death})^s \cdot (1 - 2Q(q_B))^2$and $P(A_3) = \sum_{i=0}^{s}(1 - P_{death})^i \cdot P_{death} \cdot (1 - P_{birth})^{s-i}$ (15-16). Event A_4 includes many different sequence types. e.g. D-B-ND-ND-...-ND, with probability $P_D \cdot P_B \cdot (1 - P_{ND})^{s-1}$, or ND-D-NB-...-NB-B, with probability $P_D \cdot (1-P_B)^{s-2} \cdot P_B \cdot (1-P_D)$, where B=Birth, D=Dead/Death and N=No/Not. By examining all sequence types and summing them, the corresponding probability can be written as:

$$P(A_4) = \sum_{m=0}^{s-1} \sum_{i=m}^{s-1} P_D \cdot P_B \cdot (1 - P_D)^i \cdot (1 - P_B)^{s-i-1} \quad (25)$$

However, when assumptions are reasonable (typically short sequences of 2 to 3 successive samples), P_4 is significantly lower than 0.01 and it can be neglected, so that:

$$P_{err} = \frac{P(A_2)}{P(A_2) + P(A_3)} \quad (26)$$

Finally, when substituting here the derivations for $P(A_2)$ and $P(A_3)$, (18-19) appear.

ACKNOWLEDGMENT

This work has been supported by the Spanish National Projects ELISA (TEC2014-59255-C3-3-R) and TERESA-ADA (TEC2017-90093-C3-2-R) (MINECO/AEI/FEDER, UE).

REFERENCES

[1] Z. Sheng, H. D. Tuan, H. H. Nguyen and Y. Fang, "Pilot Optimization for Estimation of High-Mobility OFDM Channels", *IEEE Trans. on Veh. Tech.*, vol. 66, no. 10, pp. 8795-8806, October 2017.

[2] W. Guo, W. Zhang and M. Pengcheng, "High-Mobility OFDM Downlink Transmission With Large-Scale Antenna Array", *IEEE Trans. on Veh. Tech.*, vol. 66, no. 9, pp. 8600-8604, September 2017.

[3] M. S. Grewal and P. A. Angus, *Kalman Filtering: Theory and Practice using MATLAB*, New York, NY, USA: Wiley, 2001.

[4] Z. Jellali and L. N. Atallah, "Fast Fading Channel Estimation by Kalman Filtering and CIR Support Tracking", *IEEE Trans. on Broadcasting*, vol. PP, no. 99, pp. 1-9, August 2017.

[5] T. Y. Al-Naffouri, "An EM-Based Forward-Backward Kalman Filter for the Estimation of Time-Variant Channels in OFDM", *IEEE Trans. on Sig. Proc.*, vol. 55, no. 7, pp. 3924-3930, July 2007.

[6] U. Güntürkün, C. Schlegel and D. Truhachev, "Compression-Aided Kalman Filter for recursive Bayesian estimation of sparse wideband channels in OFDM systems", *OCEANS 2016 MTS/IEEE Monterey*, Monterey, CA, USA, Sept. 2016, pp. 1-8.

[7] D. C. Dalwadi and H. B. Soni, "A novel channel estimation technique of MIMO-OFDM system based on Extended Kalman filter", *Proc. 2017 4th Int'l Conf. on Electr. and Comm. Systems (ICECS)*, Coimbatore, India, Feb. 2017, pp. 158 - 163.

[8] R. Zhang and W. Chen, "A mixture Kalman filter approach for blind OFDM channel estimation", *Proc. Conf. Record 38th Asilomar Conf on Signals, Systems and Computers*, vol. 1, pp. 350-354, 2004.

[9] D. Angelosante, E. Biglieri and M. Lops, "Multipath Channel Tracking in OFDM systems", *Proc. 2007 18th Int'l Symp. on Pers., Ind. and Mob. Radio Comms. (PIMRC)*, Athens, Greece, Sept. 2007, pp. 1-5.

[10] D. Angelosante, E. Biglieri and M. Lops, "Sequential Estimation of Multipath MIMO-OFDM Channels", *IEEE Trans. Signal Processing*, vol. 57, no. 8, pp. 3167-3181, March 2009.

[11] P. Z. Peebles, *Probability, Random Variables and Random Signal Principles*, New York, NY, USA: Wiley, 1987.

[12] P. Banelli, R. C. Cannizzaro and L. Rugini, "Data-Aided Kalman Tracking for Channel Estimation in Doppler-Affected OFDM Systems", *Proc. 2007 Int'l Conference on Ac., Sp. and Sig. Proc. (ICASSP)*, Honolulu, HI, USA, April 2007, vol. 3, pp. 133-136.

[13] Z. Yuanjin, "A novel channel estimation and tracking method for wireless OFDM systems based on pilots and Kalman filtering", *IEEE Trans. Consumer Electronics*, vol. 49, no. 2, pp. 275-283, May 2003.

[14] R. He, B. Ai, W. Gongpu, G. Ke, Z. Zhangdui, A. F. Molisch, C. Briso-Rodriguez and C. Oestgest, "High-Speed Railway Communications. From GSM-R to LTE-R.", *IEEE Vehicular Technology Magazine*, pp. 49-58, September 2016.

[15] B. Chen, Zh. Zhong, B. Ai, K. Guan, R. He and D. G. Michelson, "Channel Characteristics in High-Speed Railway. A Survey of Channel Propagation Properties", *IEEE Vehicular Technology Magazine*, pp. 67-78, June 2015.

[16] D. W. Matolak and R. Sun, "Unmanned Aircraft Systems. Air-Ground Channel Characterization for Future Applications", *IEEE Vehicular Technology Magazine*, pp. 79-85, June 2015.

[17] D. W. Matolak and R. Sun, "Air-Ground Channel Characterization for Unmanned Aircraft Systems Part II: Hilly and Mountainous Settings", *IEEE Trans. on Veh. Tech.*, pp. 1913-1925, June 2016.

[18] K. Mahler, W. Keusgen, F. Tufvesson, T. Zemen and G. Caire, "Measurement-Based Wideband Analysis of Dynamic Multipath Propagation in Vehicular Communication Scenarios", *IEEE Trans. on Veh. Tech.*, vol. 66, no. 6, pp. 4657-4667, June 2017.

[19] W. Zhang, F. Gao, H. Minn and H.-M. Wang, "Scattered Pilots-Based Frequency Synchronization for Multiuser OFDM Systems With Large Number of Receive Antennas", *IEEE Trans. on Comms.*, vol. 65, no. 4, pp. 1733-1745, April 2017.

[20] S. Mukherjee and S. K. Mohammed, "Constant Envelope Pilot-Based Low-Complexity CFO Estimation in Massive MU-MIMO Systems", *Proc. 2016 IEEE Global Comms. Conf. (GLOBECOM)*, Washington, DC, USA, December 2016, pp. 1-5.

[21] W. Zhang, F. Gao, S. Jin and H. Lin, "Frequency Synchronization for Uplink Massive MIMO Systems", *IEEE Trans. on Wireless Comms.*, vol. 17, no. 1, pp. 235-249, January 2018.

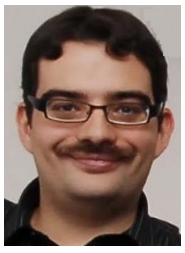

Diego Méndez-Romero received his M.Sc. degree in Mathematics and his B.Sc. in Business Sciences from the Universidad Nacional de Educación a Distancia, Spain, respectively in 2009 and 2012, and his Telecommunication System Engineering degree in 2015 from Carlos III University of Madrid (UC3M), Spain, where he currently is a PhD candidate in Multimedia and Communications. He has been working in engineering consultancy and documentation services since 2003. He co-founded the engineering-service startup Agencia de Ingeniería, where he worked as CEO from 2009 to 2013.

He is currently with the Department of Signal Theory and Communications, UC3M, Spain, as a part-time professor. He has been awarded the prestigious Spanish magazine Emprendedores' 2009 Entrepreneurship Prize, as well as the Innovation Prize from UC3M's technology start-up incubator. His research interests include multicarrier communications, channel tracking and signal processing for wireless systems.

M. Julia Fernández-Getino García (S'99 - AM'02 - M'03) received the M. Eng. and Ph.D. degrees in telecommunication engineering from the Polytechnic University of Madrid, Spain, in 1996 and 2001, respectively. She is currently with the Department of Signal Theory and Communications, Carlos III University of Madrid, Spain, as an Associate Professor. From 1996 to 2001, she held a research position with the Department of Signals, Systems and Radiocommunications, Polytechnic University of Madrid. She visited Bell Laboratories, Murray Hill, NJ, USA, in 1998; visited Lund University, Sweden, during two periods in 1999 and 2000; visited Politecnico di Torino, Italy, in 2003 and 2004; and visited Aveiro University, Portugal, in 2009 and 2010. Her research interests include multicarrier communications, coding and signal processing for wireless systems.

She received the best Master Thesis and Ph.D. Thesis awards from the Professional Association of Telecommunication Engineers of Spain in 1998 and 2003, respectively; the Student Paper Award at the IEEE International Symposium on Personal, Indoor and Mobile Radio Communications (PIMRC) in 1999; the Certificate of Appreciation at the IEEE Vehicular Technology Conference (VTC) in 2000; the Ph.D. Extraordinary Award from the Polytechnic University of Madrid in 2004; the Juan de la Cierva National Award from AENA Foundation in 2004; and the Excellence Award from Carlos III University of Madrid in 2012 for her research career.